Tellus (2008), 60A, 261–272
Printed in Singapore. All rights reserved

TELLUS

Combining the mid-latitudinal and equatorial mass/wind balance relationships in global data assimilation

By HEINER KÖRNICH* and ERLAND KÄLLÉN, *Department of Meteorology, Stockholm University, SE-10691 Stockholm, Sweden*

(Manuscript received 26 January 2007; in final form 6 July 2007)

ABSTRACT

Multivariate data assimilation is achieved by introducing mass/wind balance relationships in the background term. Geostrophy is commonly used as such a relationship in mid-latitudes. For tropical latitudes, a new balance relationship on the basis of equatorial waves has been proposed. In order to combine the equatorial with the mid-latitudinal formulation, a new data assimilation scheme is developed. The balance relationships are formulated in terms of Hough modes. For the minimization of the cost function, a control variable is constructed, where the background error is projected onto an appropriate selection of Hough modes which are weighted with their respective background covariances. The covariance structures of the data assimilation scheme are examined with single observation experiments and the increments are discussed with respect to the balance relationships. Finally, the new proposed assimilation scheme is tested in a simple observing system simulation experiment. The application of an incomplete balance relationship based on geostrophy leads to a misinterpretation of observational data and thus to enhanced analysis errors. Only the combined balance relationship improves the tropical analysis. This improvement is expected to play an important role for the analysis quality, when future wind observations from the Earth Explorer Atmospheric Dynamics Mission are available.

1. Introduction

Numerical weather prediction and climate research rely on data assimilation, since they both need the state of the atmosphere in a homogeneous physical space based on all available observations. An important impact in data assimilation results from multivariate relationships in the background error. The classically applied mass/wind relationship is geostrophy, which yields a geostrophic wind response to a mid-latitudinal temperature observation. Based on numerous space-borne temperature observations, data assimilation can reconstruct the large-scale flow in mid-latitudes. However, the usability of geostrophy breaks down in the tropical area. Furthermore, the geostrophic adjustment theory (Rossby, 1937, 1938) predicts that the wind field information determines the atmospheric state for all length scales in the tropics and also for the mesoscales in mid-latitudes. These aspects stress two problems in global data assimilation. First, global wind information is needed, and second, a balance relationship for the tropics has to be included.

The global coverage of high-quality wind observations will be provided by the Earth Explorer Atmospheric Dynamics Mission (ADM-Aeolus). The first satellite in this project is scheduled to be launched by the European Space Agency in 2009. The satellite carries a Doppler wind lidar which will retrieve the line-of-sight wind information (Stoffelen et al., 2005). Since only one component of the wind field will be available, the full wind vector has to be reconstructed using data assimilation.

A tropical mass/wind balance relationship on the basis of equatorial waves has been suggested by Žagar et al. (2004). The authors use the idealized framework of a shallow water model on an equatorial beta-plane. The respective equatorial waves are calculated as the normal modes of the linearized equations, the so-called Hough modes (e.g. Matsuno, 1966). Each mode is assigned a certain variance which is derived from observational data. This new background error formulation demonstrates that the large-scale tropical flow is indeed reconstructed, if wind observations are available. Žagar et al. (2005) applied the formulation to more realistic conditions using data from the operational model of the European Centre for Medium-range weather forecasts (ECMWF). However the tropical mass/wind balance relationship has not been tested in a global model. For example, the state-of-the-art data assimilation scheme of the ECMWF has 'virtually no balance near the equator' (Derber and Bouttier, 1999).

The analysis of tropical observations yields equatorial waves with different respective equivalent depths of the shallow water

*Corresponding author.
e-mail: heiner@misu.su.se
DOI: 10.1111/j.1600-0870.2007.00286.x

framework. Milliff and Madden (1996) used surface pressure and rawinsonde observations, while Bantzer and Wallace (1996) examined data sets from the satellite-based microwave sounding unit. Both articles report a fast ($\approx$40 m s^{-1}) eastward propagating structure which resembles a Kelvin mode with an estimated equivalent depth of 200 m. This mode agrees approximately in the phase speed and the vertical structure function with the model studies of Gill (1980). On the other hand, Wheeler and Kiladis (1999) determined the dispersion relation of different wave modes from the satellite-observed outgoing long-wave radiation. Their analysis derives Kelvin, equatorial Rossby, mixed Rossby-inertia gravity, and inertia-gravity modes. The equivalent depths range from 12 to 50 m and the authors attribute this reduced equivalent depth to convectively coupled equatorial waves.

The aim of the present work is to include the equatorial mass/wind balance relationship in a global data assimilation scheme. As noted above, the observed atmospheric flow of a given height level displays different balance relationships depending on latitude and spatial scale of the motion. The focus lies here on geostrophy for mid-latitudinal flow and convectively coupled equatorial waves. Both constraints can be expressed through the Hough modes of two different equivalent depths and their respective vertical structure functions. In order to keep the approach simple, it is appropriate to develop the new data assimilation scheme for a single layer in a global shallow water model. The properties of the data assimilation with the new cost function will be examined with two approaches. First, its response to one-point observations displays the structure of the background covariances. Here, it will be of interest to see how the different Hough modes contribute to the overall mass/wind balance relationship. Second, in an *identical twin* observing system simulation experiment, we will study both the impact of the new balance relationship compared to the conventional one and the role of particular observation types on the analysis. Especially, it will be explored how to maximize the benefit of line-of-sight wind observations as expected from the ADM-Aeolus.

The study is structured as follows. The new formulated cost function and its application to the global shallow water model is described in Section 2. The covariance structures as displayed through single point observations are examined in Section 3.1, while Section 3.2 presents the observing system simulation experiments using artificial global data. Section 4 gives concluding remarks.

2. Methods

2.1. Formulation of the cost function

In data assimilation, the available observations are combined with the a priori-knowledge of the atmosphere in order to determine the optimal estimate of the atmospheric state, that is, the analysis. The a priori-knowledge contains dynamic models and diagnostic relationships as well as the background state of the atmosphere. The solution or the increment $\delta\mathbf{x}$ is found by minimizing the cost function J in variational data assimilation, here in the 3-D variational form:

$$J(\delta\mathbf{x}) = \frac{1}{2}\delta\mathbf{x}^T\mathbf{B}^{-1}\delta\mathbf{x} + \frac{1}{2}\left[\mathbf{y} - H\left(\mathbf{x_b} + \delta\mathbf{x}\right)\right]^T\mathbf{R}^{-1}\left[\mathbf{y} - H\left(\mathbf{x_b} + \delta\mathbf{x}\right)\right], \quad (1)$$

where $\mathbf{x_b}$ is the background state in model space, $\mathbf{y}$ the vector of observations, H the forward model projecting the model state vector into the observational space, $\mathbf{R}$ and $\mathbf{B}$ represent the covariance matrices of the observation error and of the background error, which is the difference between the background and the true state $\mathbf{x_t}$:

$$\epsilon_b = \mathbf{x_b} - \mathbf{x_t}. \quad (2)$$

The second term in eq. (1) weights the difference between the analysis and the observations with the observation error covariance. The first term in eq. (1) is the so-called background term describing the a priori-knowledge. It is responsible for spatial spreading of the observational information and for transforming information between different variables using multivariate balance relationships. Since the background error covariance matrix $\mathbf{B}$ is non-diagonal and has usually dimensions of several hundred thousands and more, its inversion is technically impossible. One way to solve this problem is to introduce a so-called control variable. This is done by transforming the increment $\delta\mathbf{x}$ into a space spanned by the rows of the matrix $\mathbf{L}$ where $(\mathbf{L}^T\mathbf{L}) = \mathbf{B}^{-1}$. Then the first term on the r.h.s. of eq. (1) becomes simply a quadratic term of the control variable χ which implies that numerical minimization of the cost function becomes feasible.

The balance relationships in this study are formulated in terms of Hough modes. The respective Hough modes are calculated globally as the normal modes of the linearized shallow water equations (Daley, 1991). The link to the full 3-D atmosphere is given by the linearization of the primitive equations around a state of rest. This yields horizontal and vertical structure equations with equivalent depth as the separation constant. The horizontal structure equations correspond to the shallow water equations, while the equivalent depth determines the respective vertical structure function for each set of Hough modes. The mid-latitudinal balance relationship is now implemented in the background error through the Hough modes with an equivalent depth of 10 000 m, that is, the vertical structure function is deep barotropic. For the tropical balance relationship, Hough modes with an equivalent depth of 25 m are used in accordance with the observations of convectively coupled equatorial waves (Wheeler and Kiladis, 1999). For the respective vertical structure function, it has to be taken into account that these waves are described by a different set of equations, since the process of convection is included here. Convection is reducing the stability and thus the equivalent depth (Lindzen, 1974). The vertical scale is assumed to be determined by the vertical extension of

the convective heating (Gill, 1980). Wheeler et al. (2000) derive a vertical wavelength of about 10 km for the equatorial modes.

In order to select the Hough modes of interest, a frequency criterion is applied following Žagar et al. (2004). Therein, all modes with periods shorter than about 6 hours are rejected. For the Hough modes with equivalent depth of 10 000 m, this selection means that only Rossby and the westward propagating Rossby-gravity mode are included in the mid-latitudinal balance relationship which represents quasi-geostrophic balance. In addition to the frequency criterion, for the Hough modes with equivalent depth of 25 m all Rossby modes with meridional wavenumbers $n > 2$ and all eastward inertia-gravity modes with $n > 0$ are excluded, since tropical observations do not show these higher modes (Wheeler and Kiladis, 1999). These restrictions ensure also that only equatorially trapped modes contribute to the tropical balance relationship. The included Hough modes with an equivalent depth of 25 m are westward inertia-gravity, Rossby, mixed Rossby-gravity, Kelvin, and eastward inertia-gravity (only $n = 0$) modes. In the following we will call these modes shortly equatorial Hough modes, while the deep barotropic Rossby modes based on an equivalent depth of 10 000 m are named mid-latitudinal Hough modes.

The number of Hough modes which are applied in the balance relationship depends on the resolution of the model. As described in Section 2.2, a global, spectral shallow-water model will be used at a spectral resolution of T42. At this resolution, the model contains 5544 degrees of freedom, whereas the total number of Hough modes adds up to 2150 with 346 equatorial modes.

At this point, it should be noted that the Hough modes for mid-latitudes and Tropics with equivalent depths of 10 000 and 25 m are both global modes and that, although given the equivalent depth each set of modes is orthogonal, the two sets are non-orthogonal. For example, both sets include a Rossby wave with meridional and zonal wavenumber equals one. These Rossby modes have a different meridional extent, but nevertheless correlate strongly. This remains also valid, even if the vertical-structure function is taken into account, since only the equatorial modes include the interaction with convection.

In order to construct a background error with both mid-latitudinal and equatorial balance relationship, the increment $\delta\mathbf{x}$ is separated into two components, one described by mid-latitudinal modes and one by equatorial modes. For each, a separate control variable is formulated:

$$\delta\mathbf{x} = \delta\mathbf{x}_m + \delta\mathbf{x}_e \tag{3}$$

$$\begin{pmatrix} \chi_m \\ \chi_e \end{pmatrix} = \begin{pmatrix} \mathbf{L_m} & 0 \\ 0 & \mathbf{L_e} \end{pmatrix} \begin{pmatrix} \delta\mathbf{x}_m \\ \delta\mathbf{x}_e \end{pmatrix} \tag{4}$$

with

$$\mathbf{L_{m/e}} = \mathbf{D_{m/e}}\mathbf{M^T_{m/e}}. \tag{5}$$

Each increment is projected on the respective selection of Hough modes which represent the mid-latitudinal (**m**) or equatorial (**e**) balance relationship. The matrices $\mathbf{M_{m/e}}$ consist of the Hough modes in their columns. Then, each component of the control vector is weighted with the standard deviation of the Hough mode by multiplication with the diagonal matrices $\mathbf{D_{m/e}}$. The Hough mode variances yield the contribution of each mode to the background error covariance. To achieve a diagonal background covariance matrix, it is assumed that the time series of the Hough modes for mid-latitudes and Tropics are uncorrelated.

Using the control variable, the cost function can be written as

$$\begin{aligned} J(\chi_m, \chi_e) = {} & \frac{1}{2}\chi_m^T\chi_m + \frac{1}{2}\chi_e^T\chi_e \\ & + \frac{1}{2}\left[\mathbf{y} - H\left(\mathbf{x_b} + \mathbf{L_m}^{-1}\chi_m + \mathbf{L_e}^{-1}\chi_e\right)\right]^T \\ & \times \mathbf{R}^{-1}\left[\mathbf{y} - H\left(\mathbf{x_b} + \mathbf{L_m}^{-1}\chi_m + \mathbf{L_e}^{-1}\chi_e\right)\right]. \end{aligned} \tag{6}$$

The first and second term on the r.h.s. of eq. (6) are the background term, now separated for the mid-latitudinal and equatorial control variable. The third term on the r.h.s. is the observation term, in which both increments $\delta\mathbf{x}_m$ and $\delta\mathbf{x}_e$ are combined, so that double-counting the observational information is avoided.

For the minimization of the new cost function in eq. (6), the function has to be differentiated with respect to the control vector (χ_m, χ_e):

$$\nabla_{\chi_m} J = \chi_m - \mathbf{L_m}^{-T}\mathbf{H}^T\mathbf{R}^{-1}\left[\mathbf{y} - H(\mathbf{x_b} + \mathbf{L_m}^{-1}\chi_m + \mathbf{L_e}^{-1}\chi_e)\right] \tag{7}$$

$$\nabla_{\chi_e} J = \chi_e - \mathbf{L_e}^{-T}\mathbf{H}^T\mathbf{R}^{-1}\left[\mathbf{y} - H(\mathbf{x_b} + \mathbf{L_m}^{-1}\chi_m + \mathbf{L_e}^{-1}\chi_e)\right]. \tag{8}$$

In eq. (6), the background term is reformulated in terms of a selection of mid-latitudinal and equatorial Hough modes, which serve as mass–wind balance relationships. The background error covariance matrix is now expressed through the variances of the modes in the weighting matrices $\mathbf{D_{m/e}}$. In order to specify these variances, the variance distribution of the Hough modes in the background error has to be determined, that is, the background error has to be projected onto the Hough modes. However, the background error is normally unknown, since we do not know the true state of the atmosphere. Common circumventions are using different estimates for the background error which are assumed to describe the same statistical behavior, for example, differences between different forecast times (Parrish and Derber, 1992) or differences between forecasts of ensemble members (Fisher, 2003). For the current study, the variance distribution of the Hough modes is prescribed as a red spectrum defined in eq. (11).

Assuming that the background error is given, the non-orthogonality of the convectively coupled equatorial and the mid-latitudinal Hough modes poses a problem, since the projection of the background error on these modes is not uniquely determined. Here, the following approach is used: An optimal projection is sought by minimizing the error $\mathcal{E}$ between the

background error and its projection on the Hough modes:

$$\mathcal{E} = \|(\mathbf{x_b} - \mathbf{x_t}) - \mathbf{M_m a_m} - \mathbf{M_e a_e}\|^2 , \tag{9}$$

where the vectors $\mathbf{a_{m/e}}$ represent the amplitudes for the different Hough modes and the energy norm of the shallow water system (Kasahara, 1976) is used. Since the energy norm depends on the value of the equivalent depth and, here, two different depths are combined, the norm incorporates their mean value. This approximation is a possible error source during the estimation of the Hough mode variances.

In the current work, eq. (9) is minimized numerically using the gradient of the error function:

$$\nabla_{\mathbf{a_{m/e}}}\mathcal{E} = -2\mathbf{M_{m/e}}^T \|(\mathbf{x_b} - \mathbf{x_t}) - \mathbf{M_m a_m} - \mathbf{M_e a_e}\| . \tag{10}$$

This minimization is carried out for each available time step, so that the standard deviations of the amplitudes $\mathbf{a_{m/e}}$ yield the input for the weighting matrices $\mathbf{D_{m/e}}$. An important issue for the minimization of eq. (9) is its well posedness which can only be ensured, if the number of degrees of freedom for the background error is equal or larger than the total number of considered Hough modes in the matrices $\mathbf{M_m}$ and $\mathbf{M_e}$, and if all Hough modes are linearly independent. The applied selection rules allow only for the slow Rossby modes in the mid-latitudes, which yield one third of the degrees of freedom for a given spectral resolution. The number of allowed equatorial Hough modes is even lower due to the more restrictive selection rule of equatorially trapped modes. Additionally, the Hough modes for the different equivalent depths are checked to be linearly independent. Thus, the minimization of eq. (9) is a well-posed problem.

2.2. Simulations in a global shallow water model

The combination of equatorial and mid-latitudinal balance relationships can be tested with data assimilation experiments using a global shallow water model. The applied global shallow water model is based on the dynamical core of the Kühlungsborn Mechanistic general Circulation Model (Becker and Schmitz, 2001). For the current task the model equations have been reduced to the shallow water equations. The model is spectral and no friction or diffusion is taken into account. A resolution of triangular truncation at total wavenumber 42 is used.

Variational data assimilation is carried out minimizing the cost function in eq. (6), where the vector $\mathbf{x_b}$ and accordingly the increment $\delta\mathbf{x}$ and the transformation matrices $\mathbf{L_{m/e}}$ are expressed in spectral coordinates. All observations $\mathbf{y}$ are chosen to lie on the equivalent Gaussian grid of the model, which is used for the transformation between spectral and grid space. Finally, the minimization is done using the minimization routine M1QN3 (Gilbert and Lemaréchal, 1989). Two stopping criteria were used: the absolute precision of the cost function and the relative precision of its gradient were required to be 1×10^{-5} and 1×10^{-3}, respectively.

For the background term, the variances of each Hough mode which go into the matrices $\mathbf{D_{m/e}}$ have to be defined. In the current study, a spectral variance distribution γ_h^2 is chosen as in Žagar et al. (2004):

$$\gamma_h^2(K) = \frac{\Gamma_h^2}{[1 + \ell^2(K)^2]^2}, \tag{11}$$

where Γ_h^2 determines the total variance of the specific mode, and h indicates the different mode types. The horizontal scale ℓ, which is set to a value of 0.1, affects the slope of the variance spectrum. The 1-D wavenumber K enables atmospheric anisotropy (Kasahara, 1976):

$$K = \sqrt{(c_1 k)^2 + (c_2 n)^2} \tag{12}$$

with zonal and meridional wavenumbers k and n. The tunable constants c_1 and c_2 are here chosen to be 2 and 1, which means that the variance of the mode decreases stronger with increasing meridional than with increasing zonal wavenumber. This choice leads to covariance patterns which are elongated in the zonal direction. The inverse of γ_h is directly used in the matrices $\mathbf{D_{m/e}}$.

The total variance for mid-latitudinal and equatorial Hough modes are determined such that the background errors in the wind have globally a magnitude of a few meters per second. Due to this, the total variance of the mid-latitudinal modes is 10 times larger than the equatorial ones. The relative variances in the equatorial background error are chosen, respectively as 7, 33, 15, 37 and 7% for westward inertia-gravity, westward mixed Rossby-inertia gravity, Rossby, Kelvin and eastward inertia-gravity modes.

3. Results

3.1. One-point observations

The response of the new cost function from eq. (6) to one-point observations displays the structure of the background covariances, and thus the mass/wind balance relationships used during the data assimilation. It will be of interest to see how the different mid-latitudinal and equatorial Hough modes contribute to the balance relationship at different latitudes. Therefore, we will explore the response to single observations at the equator, slightly off the equator and in mid-latitudes. The focus lies especially on the Tropics where both equatorial and mid-latitudinal Hough modes can contribute. In this region, it is important to avoid a double-counting of the observational information.

Figure 1 shows the increments to a single zonal wind observation of 3 ms^{-1} at 29.3°N 0°E, 9.8°N 0°E and 1.4°N 0°E. The analysis increments are separated here into the contribution of the mid-latitudinal and equatorial Hough modes which are displayed in the left- and right-hand panels of Fig. 1, respectively. For the mid-latitudinal single-point observation (Figs. 1a and b) the covariance structure is solely determined by the mid-latitudinal Rossby modes (Fig. 1a), whereas the contribution of the equatorial modes is negligible (Fig. 1b), since the convectively coupled

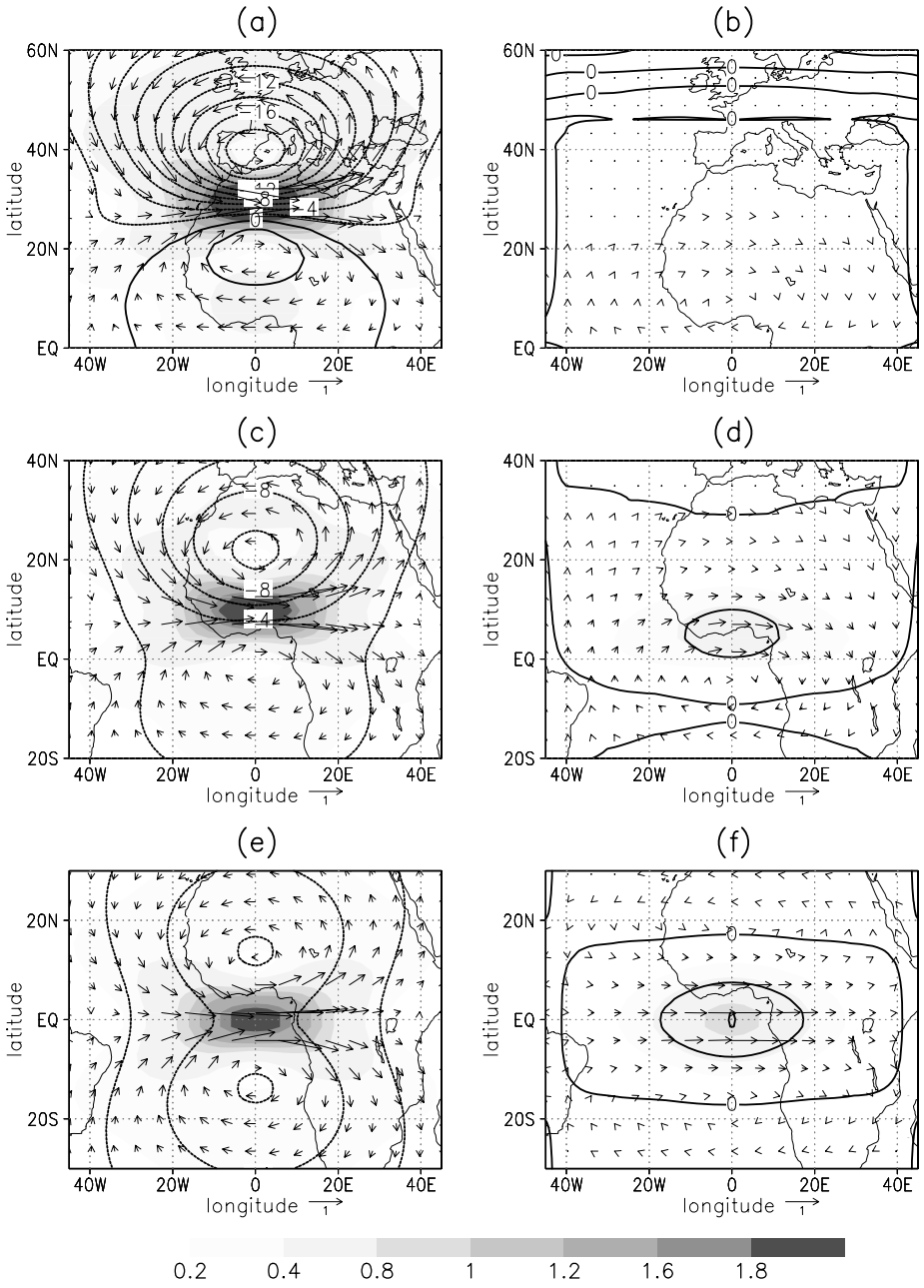

Fig. 1. Latitude–longitude plot of the increment to a single zonal wind observation at 29.3°N 0°E (a, b), 9.8°N 0°E (c,d), and 1.4°N 0°E (e, f). The increment is split into the contributions of mid-latitudinal (a, c, e) and equatorial (b, d, f) Hough modes. The contours show the geopotential height with a contour interval of 2 m in (a, c, e) and 0.5 m in (b, d, f). Arrows represent the wind field with the corresponding wind vector in ms^{-1} plotted below each panel. The magnitude of the wind field is shaded in ms^{-1}.

equatorial modes do not include significant amplitudes in mid-latitudes. Therefore, the increment for the observation at 29.3°N reflects the geostrophic balance relationship and it corresponds to the result of Derber and Bouttier (1999, their fig. 16).

When the observation is situated closer to the equator, the contribution of the equatorial background term increases. For the single zonal wind observation at 9.8°N (Figs. 1c and d), the mid-latitudinal contribution gets weaker than for the observation at 29.3°N, while the increment by the equatorial modes shows clearly non-geostrophic contributions due to a mixture of the Kelvin and the mixed Rossby-inertia gravity modes.

The increment to the equatorial zonal wind observation at 1.4°N (Figs. 1e and f) displays an even more reduced impact of the mid-latitudinal Rossby modes. There, the equatorial modes

produces a distinct structure in form of an equatorially trapped Kelvin wave with non-geostrophic wind crossing the height isolines. However its geopotential component is strongly reduced due to impact of equatorial Rossby modes. This compensation between Kelvin and Rossby modes for equatorial zonal wind observations was already described in Žagar et al. (2004).

Additionally, in the presented setup of the spectral variance distributions, the increment is always strongly dominated by mid-latitudinal Rossby modes with low total wavenumbers, for example, for the equatorial zonal wind observation the mode with meridional wavenumber one (Fig. 1e). This feature is not realistic, since a strong impact of barotropic Rossby modes on the equatorial dynamics is not observed. Nevertheless, the spectral variance distribution is used for the sake of simplicity.

The increments to a single equatorial observation of the meridional wind with a value of 3 ms^{-1} and to a single geopotential-height observation with a value of 3 m is shown in Fig. 2. The impact of the equatorial Hough modes is especially strong in the response to the single meridional wind observation (Fig. 2b). The response resembles the equatorial mixed Rossby-inertia gravity mode, which dominates the total wind increment in the Tropics, whereas the contribution of the mid-latitudinal Hough modes is small (Fig. 2a). For the single geopotential observation, the increment is dominated by a mid-latitudinal Rossby mode (Fig. 2c), while the equatorial modes contribute with a weak Kelvin mode signature (Fig. 2d). Here, the mid-latitudinal Rossby and equatorial Kelvin modes compensate slightly in the zonal wind response, while the geopotential increments add up.

In order to check that observation information is not doubly counted, we examine now the case of a cost function containing only one balance relationship, that is, only geostrophy or only convectively coupled equatorial waves, thus all terms with either χ_e or χ_m are removed from eq. (6). The respective increments (Figs. 3a and b) show the same structure as for the combined background error (Figs. 1e and f), but with a far larger amplitude. If only mid-latitudinal Hough modes are taken into account, the relation between the background and observation error is approximately kept constant, since the variances of the equatorial modes is 10 times smaller than that of the mid-latitudinal modes. Therefore, the mid-latitudinal modes in

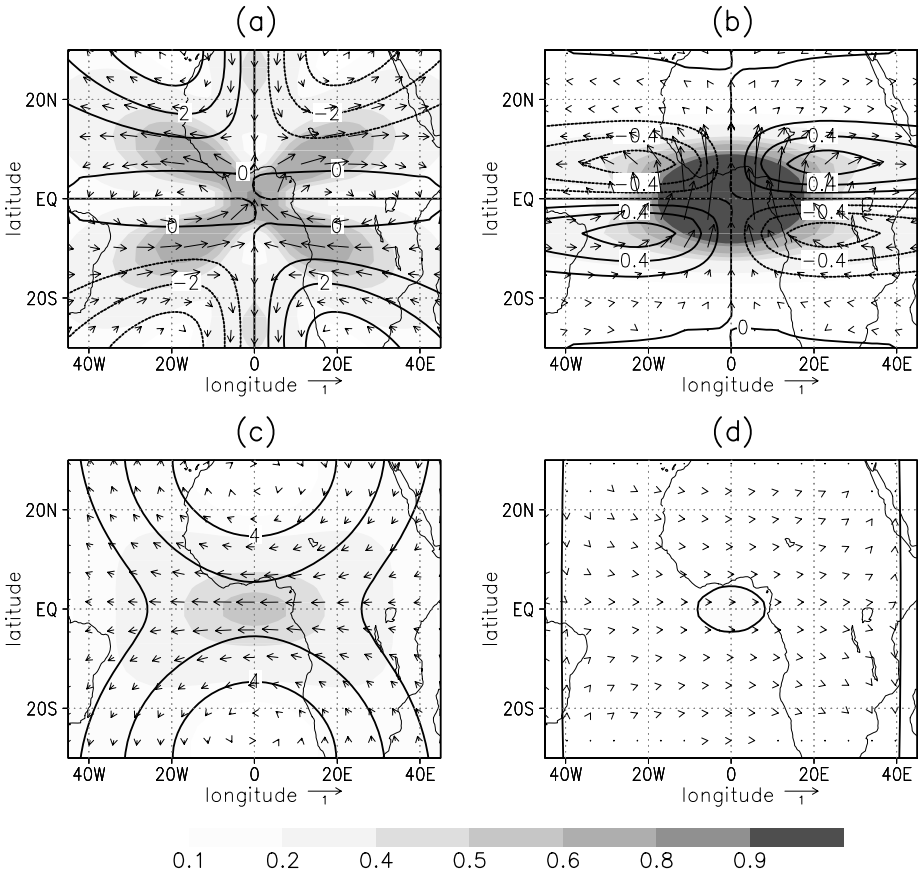

Fig. 2. Latitude–longitude plot of the increment to a single meridional wind observation (a, b) and a single geopotential observations (c, d) at 1.4°N 0°E. The increment is split into the contributions of mid-latitudinal (a, c) and equatorial (b,d) Hough modes. The contours show the geopotential height with an interval of 1 m in (a, c) and 0.2 m in (b, d). Arrows represent the wind field with the corresponding wind vector in ms^{-1} plotted below each panel. The magnitude of the wind field is shaded in ms^{-1}.

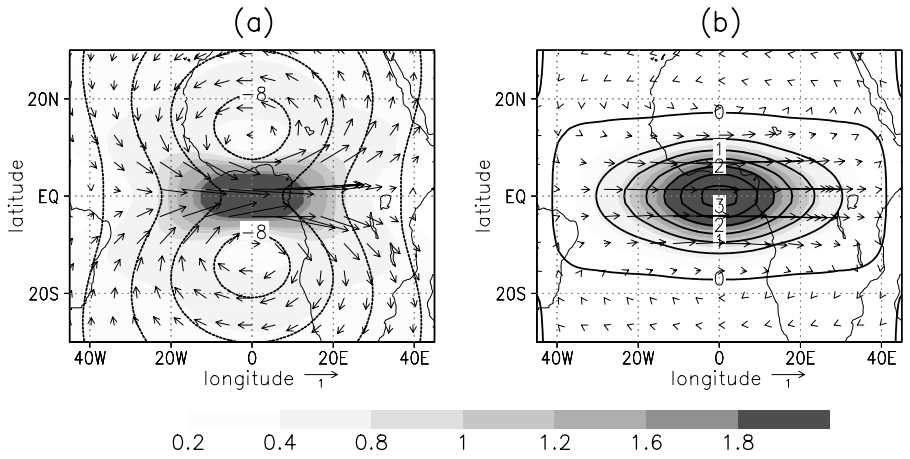

Fig. 3. Latitude–longitude plot of the increment to a single zonal wind observation at 1.4°N 0°E. During the data assimilation, only the mid-latitudinal (a) or equatorial (b) Hough modes are used in the cost function. The contours show the geopotential height with an interval of 2 m in (a) and 0.5 m in (b). Arrows represent the wind field with the corresponding wind vector in ms^{-1} plotted below each panel. The magnitude of the wind field is shaded in ms^{-1}.

Fig. 3a take over the part of the zonal wind increment which was described by the equatorial modes (Fig. 1f), so that the total zonal wind increment at the observation point remains roughly constant at 2.9 ms^{-1} . If only equatorial modes are used (Fig. 3b), the total background error is reduced, which results in a weaker total zonal wind increment at observation point with 2.8 ms^{-1} . As demonstrated, the combined background error enables the data assimilation to split the observational information into contributions of the mid-latitudinal and the equatorial balance relationship without double-counting the actual information content.

3.2. Application to global data

In an *identical twin* observing system simulation experiment, we will now assess the impact of the new balance relationship compared to the conventional one which includes only the mid-latitudinal balance relationship. Furthermore, it will be explored how particular observation types affect the quality of the analysis and how to maximize the benefit of zonal wind observations as expected from the ADM-Aeolus.

First of all, artificial data on the shallow water globe are created. This is achieved by using random amplitudes of the mid-latitudinal and equatorial Hough modes selected in Section 2.1 at a given spectral variance distribution γ from eq. (11). The relative variance distribution among the equatorial modes is the same as in Section 2.1, with the total variance of the mid-latitudinal barotropic Rossby modes being 10 times larger than that of the equatorial Hough modes. An example of this artificial data is displayed for an arbitrary longitude–latitude section in Fig. 5a. The flow shows geostrophic structures in the Extratropics and non-geostrophic behavior with flow crossing geopotential isolines in the Tropics, especially around the longitudes 20°E and 100°E.

The next task is the reconstruction of the variance distribution for the Hough modes. The background error is equal to the artificial data, since the background state in the 3-D variational data assimilation will be the resting atmosphere. For the reconstruction we will use 500 realizations of the artificial data, but also other data with the same statistical properties in respect to the Hough modes could serve. The minimization of the error in eq. (9) yields the time series of the Hough mode amplitudes which are used to derive the spectral variance distributions. These empirical distributions are generally well comparable with the analytical spectra from eq. (11) (Fig. 4). The largest differences occur for the reconstructed variances of the equatorial mixed Rossby-inertia gravity modes (black squares in Fig. 4a) underestimating the true value by up to 30% and for the reconstructed variances of the equatorial Rossby modes with a slight overestimation. These discrepancies can result either from the non-orthogonality of the two sets of Hough modes or from the approximation of the equivalent depth in the energy norm of eq. (9). As we will however see in the assimilation experiments, these differences in the variances have only a minor effect on the analysis.

Several data assimilation experiments are carried out, where different background error formulations are used, that is, the new formulation including both equatorial and mid-latitudinal balance relationship with either the analytical or the empirical variance distribution, and, on the other, the conventional formulation including only the mid-latitudinal balance relationship along with the analytical variance distribution. The observation points are randomly distributed over the globe, but in order to avoid interpolation they lie on the Gaussian grid which is equivalent to the spectral resolution of T42. The total number of grid points is 8192. Gaussian distributed random errors of 0.5 ms^{-1} for the wind observations and of 5 m for the geopotential height observations are used.

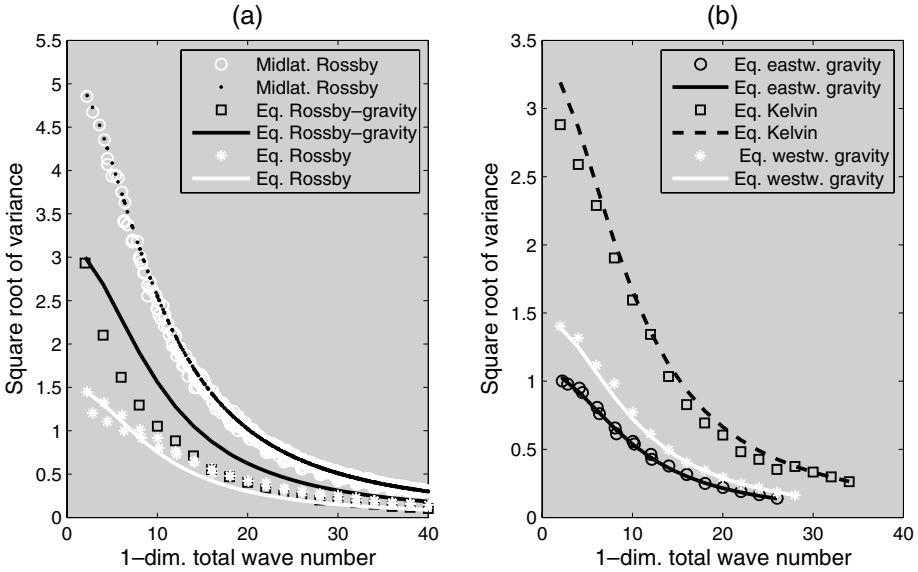

Fig. 4. Square root of spectral variance distribution for mid-latitudinal and equatorial Hough modes. The analytical variance distribution from eq. (11) is marked with dots for the mid-latitudinal Rossby modes and otherwise with lines. The symbols show the empirically derived variances for the different mode types which are denoted in the legends. The 1-D wavenumber on the x-axis is defined through eq. (12).

The analysis errors using different balance relationships for 1000 observations of geopotential and zonal wind are displayed in Figs. 5b–d. When the analytical variance distributions of both mid-latitudinal and equatorial Hough modes are used, the analysis error is smallest and covers equally Tropics as well as the mid-latitudes (Fig. 5b). The analysis error results here from missing observations and the error in the observation itself. Using the empirically reconstructed variances the analysis error (Fig. 5c) is almost the same as for the analytical variances. Small differences are visible for the winds at 0°N 60°E, where the error in the derived variances amplifies the analysis error. However, the largest analysis error occurs in the assimilation with only the mid-latitudinal Hough modes in the background error (Fig. 5d). Comparing with the best case in Fig. 5b the analysis error worsens only in the tropical area, where the correct mass/wind balance relationship is missing. Thus, this data assimilation cannot reproduce the tropical non-geostrophic structures, and additionally, it applies falsely the mid-latitudinal balance relationship for the tropical observations. It should be noted that the mid-latitudinal relationship is not wrong for the tropical region, since it is included in the artificial data, but it is not complete.

In order to quantify the results of the data assimilation experiments we examine now the root mean square errors (RMS) of the increments in the tropical and extratropical mean. Figure 6 displays the RMS as a function of the number of observations for two different data assimilation schemes: one with the new cost function from eq. (6) using both equatorial and mid-latitudinal Hough modes (lines) and one scheme with the conventional approach including only geostrophy, here in the form of mid-latitudinal Hough modes (symbols). The RMS is calculated as the mean over 20 different realizations of random data. For the assimilation scheme with mid-latitudinal Hough modes alone, the analytical Hough mode variances are applied, while the empirically derived values are used for the new complete assimilation scheme. If these values in the latter case are replaced with the analytical variances, the results of the RMS lie indistinguishably on top of the case with the empirical values (not shown). Thus, the conclusion is that the differences between the analytical and empirical variances are negligible for the data assimilation, at least for spatial means.

The performance of the new data assimilation scheme is now explored in more detail (lines in Fig. 6). First, it is determined how well the data assimilation reproduces the observed variable. As can be seen for zonal wind observations (black solid in Figs. 6a and d) as well as geopotential observations (white solid in Figs. 6c and f), the analysis performs well as regards the observed variable. Adding information in form of zonal wind or geopotential observations (white dash–dotted in Fig. 6) improves the readily observed variable only slightly. Nevertheless, balance relationships are needed especially for the non-observed variables, for example, the meridional wind for all cases.

As expected, the geopotential observations provide most information for the Extratropics (Figs. 6d–f), while zonal wind observations alone yield higher RMS values. Interestingly, this is also true for the RMS of the zonal wind itself at observation numbers lower than 1000 (Fig. 6d). The reason for it is that the large-scale geostrophic flow is better described by the geopotential than by one wind component. Combining geopotential with wind observations improves the extratropical RMS slightly.

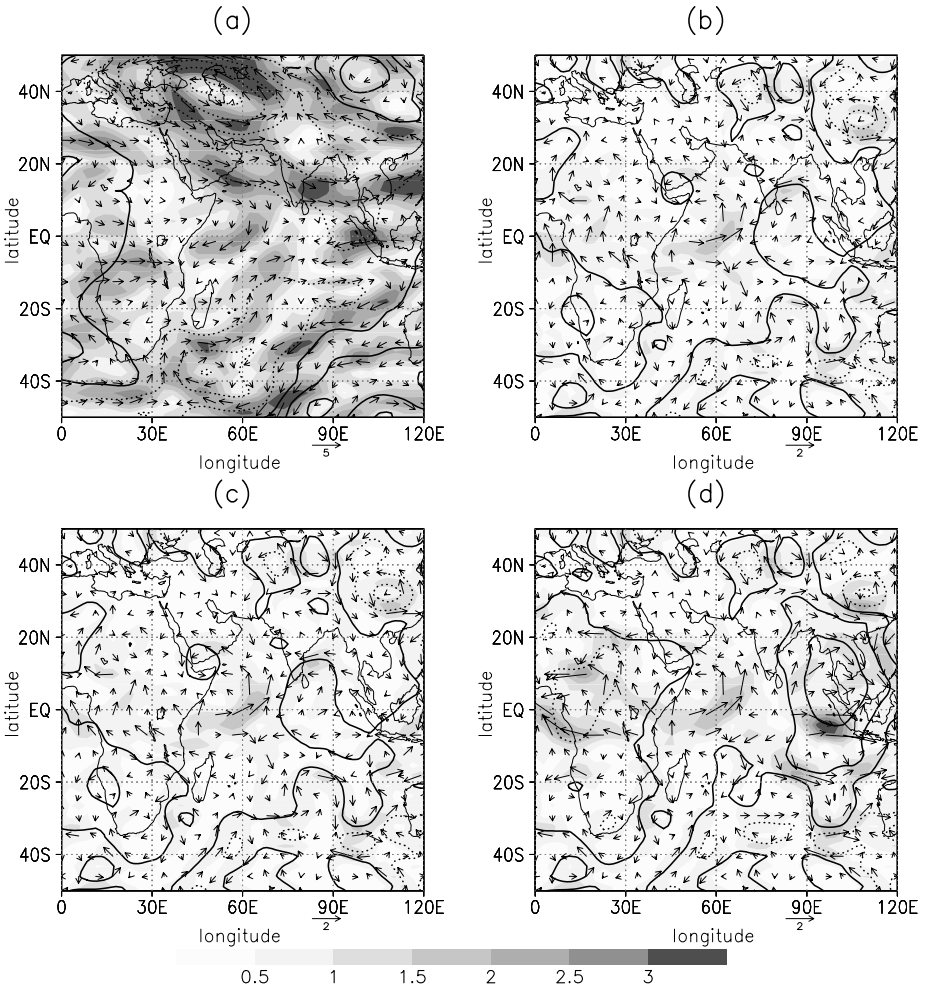

Fig. 5. Example for data assimilation of artificial data with 1000 observations of geopotential and zonal wind. (a) Truth state, (b,c) analysis error (analysis minus truth) applying the new formulated cost function with (b) the analytical or (c) the empirical variance distribution. (d) analysis error using the formulation with only the mid-latitudinal Hough modes and their analytical variance distribution. The contours show the geopotential height with an interval of 10 m in (a), and 3 m in (b–d) with negative contours being dotted. Arrows represent the wind field. The corresponding wind vector in ms^{-1} is plotted below. Shadings represent the magnitude of the wind field in ms^{-1}.

The key differences for the simulations appear in the RMS of the Tropics (Figs. 6a–c). There, the geopotential observations alone hardly reduce the RMS in the zonal and meridional wind (white solid in Figs. 6a and b). This reflects the argument of the Rossby deformation radius being very large in the Tropics and thus, the dynamics are determined by the wind information and not by geopotential information. Consequently, zonal wind observations alone yield lower RMS in the geopotential than vice versa (Figs. 6a and c). Again, the combination of geopotential with zonal wind observations improves the RMS of the non-observed variable, the meridional wind, further (Fig. 6b), as has been noted by Žagar et al. (2004). Note that this gain for the combined observations is larger in the tropical than in the extratropical region owing to the dominance of the geopotential for the geostrophic flow. Nevertheless, the combination lowers also the extratropical RMS of the observed variables compared to the cases, when only a single observation type is given (white dash–dotted against black and white solid line in Figs. 6d and f, respectively).

Finally, it is examined how the new cost function including equatorial wave modes (lines) impacts the analysis compared to the conventional case with only geostrophy (symbols in Fig. 6). In all panels, the RMS of the conventional approach lies higher than the RMS of the new cost function. For geopotential observations alone (white solid and white circles in Fig. 6), the difference between the assimilation schemes is small, because even with the new scheme, the geopotential is unable to describe the non-geostrophic tropical dynamics. This fact gives rise to the relative flat white solid curves in Figs. 6a and b. Thus, the global RMS of the wind field, which is the sum of the tropical and

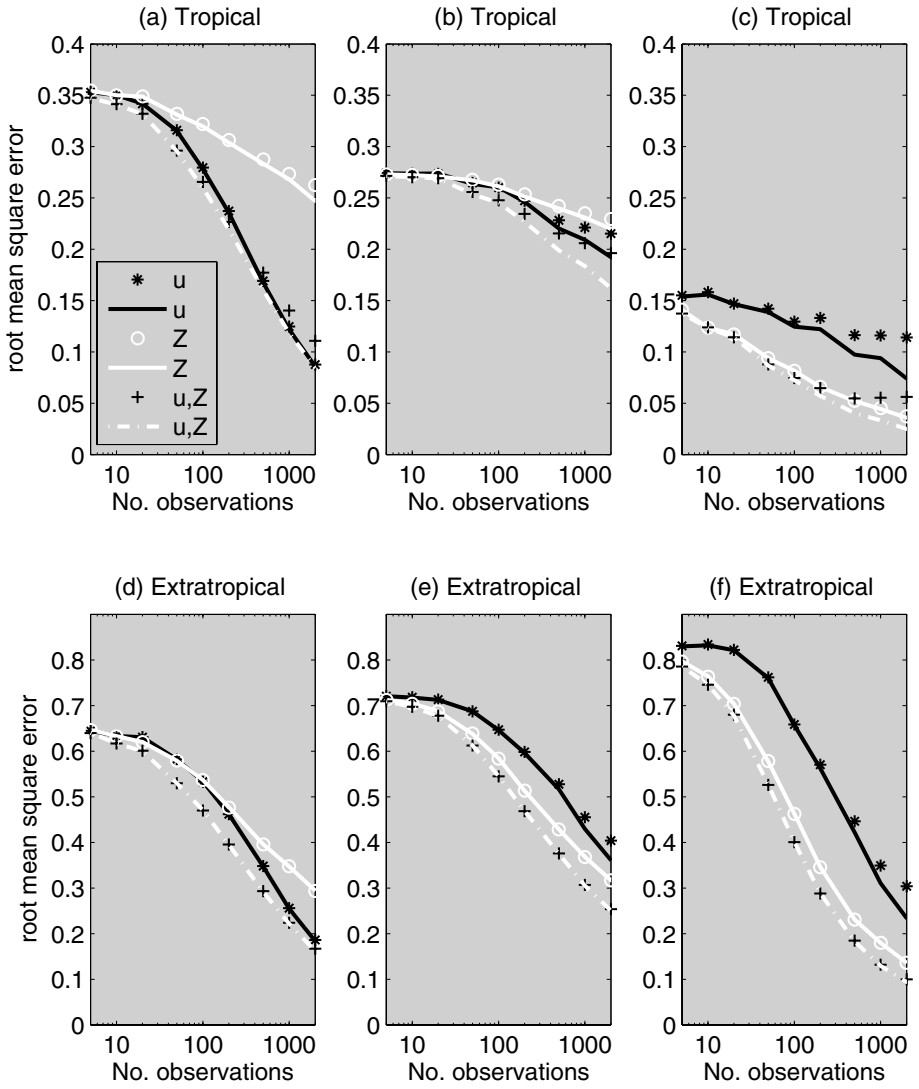

Fig. 6. Root mean square error (RMS) for zonal wind (a,d), meridional wind (b,e), and geopotential (c,f) of analysis increments as a function of number of observations. Panels (a–c) display the tropical RMS (20°S–20°N), and panels (d–f) extratropical RMS (global minus tropical). Lines represent data assimilation with both equatorial and mid-latitudinal Hough modes, while assimilations with only mid-latitudinal modes are marked with symbols. The respective observation type for each line or symbol is explained in the legend of panel (a). All values are normalized with the global RMS of the background field.

extratropical RMS, is based at high observation numbers mostly on the contribution of the tropical RMS (compare Figs. 6a,b and d,e).

As noted before, the zonal wind observations (black solid in Fig. 6) perform better for the tropical analysis of the non-observed variables than geopotential observations. If only mid-latitudinal Hough modes are used in the background term (black stars in Fig. 6), the tropical RMS of the geopotential becomes flat and particularly large, which stresses that the mid-latitudinal balance relationship is not appropriate for tropical analysis. However, the tropical RMS of the geopotential is already relatively low, since most geopotential variations occur in Extratropics.

For observations of both zonal wind and geopotential, the analysis yields the lowest RMS, if applied with the new assimilation scheme (white dash–dotted in Fig. 6). Again the combination improves even the RMS in the observed variables. This is however only true, if the new cost function is used. If only mid-latitudinal Hough modes are included in the background term (black crosses), the added observational information worsens the tropical analysis compared to the cases with only one type of observations (black crosses against black and white solid curve in Figs. 6a and c, respectively). The effect of the incomplete balance relationship is that the additional information by geopotential or zonal wind is interpreted erroneously in terms

of geostrophy and thereby it gives rise to larger tropical RMS. Therefore, an univariate analysis of the observed variable gives smaller RMS than an incomplete mass/wind balance relationship, even though the original data does contain the geostrophic relationship also in the Tropics. Nevertheless, the application of the correct balance relationship gives further improvement of the RMS, especially in the non-observed variable (white dash–dotted in Fig. 6b).

4. Concluding remarks

Balance relationships are applied in data assimilation as multivariate constraints and as a possibility to derive non-observed variables. The new data assimilation formulation combines two mass/wind balance relationships, namely geostrophy and convectively coupled equatorial waves. This combination enables a multivariate assimilation in the Tropics. It has been demonstrated that this formulation improves the usage of zonal wind observations in data assimilation, especially for the non-geostrophic tropical dynamics.

Using the incomplete mid-latitudinal balance relationship in the Tropics yields higher RMS than applying only univariate data assimilation (Fig. 6). However, current data assimilation system attribute also some variance of the background error to an *unbalanced* component (e.g. Derber and Bouttier, 1999). In such systems, the unbalanced component plays an important role in the Tropics, where the quasi-geostrophic balance relationship breaks down and the analysis becomes effectively univariate. Thus, the unbalanced component ensures that the tropical analysis does not get 'contaminated' by an inappropriate balance relationship. If an unbalanced part was introduced in the presented data assimilation with only mid-latitudinal balance, this would mean that the RMS in the case of both wind and geopotential observations would lie approximately on the same level as for the analysis with only the single observed variable, that is, the RMS for the black crosses would be lowered to the black stars and white circles in Figs. 6a and c, respectively. Nevertheless, the analysis benefits from the usage of an appropriate equatorial balance relationship.

The next step will be the inclusion of the vertical coordinate for the new data assimilation scheme. The vertical extension of the equatorial balance relationship has already been demonstrated using the ECMWF's 4-D variational system in Žagar et al. (2005). For each equatorial mode, the vertical correlation was determined on basis of tropical short-range forecast errors. This approach can also be applied in a global data assimilation, which combines tropical and mid-latitudinal balance relationships.

In the presented assimilation scheme, the mid-latitudinal balance relationship was formulated with highly barotropic Rossby modes. A more realistic representation of the background error including also baroclinic Rossby modes yields a better approximation, particularly in the subtropical transition region between mid-latitudinal and tropical dynamics. At the same time, this improvement will yield more problems in determining the equatorial Hough mode variances owing to the non-orthogonality of the chosen basis functions. Another possibility for the quasi-geostrophic balance relationship is the usage of relative vorticity as a balanced variable with the linear-balance equation where the coefficients are derived empirically (Derber and Bouttier, 1999). This approach requires a different reconstruction method than the presented one to distribute the background covariance to the different balance relationships. The easiest solution would be to first determine the variances of the equatorial modes, and to then remove their contribution from the background error before deriving the covariances with the vorticity.

The launch of ADM-Aeolus will provide dense line-of-sight wind observation with global coverage. In order to make best use of the data, it will be important to prepare the data assimilation systems for this new kind of data. One useful step will be the implementation of the mass/wind balance relationship based on equatorial waves in global data assimilation schemes.

5. Acknowledgments

The authors like to thank Nils Gustafsson for fruitful discussions. Constructive comments from two anonymous reviewers were appreciated. Several figures were produced with the free software GrADS (Grid Analysis and Display System). This work has been sponsored by the Swedish National Space Board (research contract 124/05).

References

Bantzer, C. H. and Wallace, J. M. 1996. Intraseasonal variability in tropical mean temperature and precipitation and their relation to the tropical 40–50 day oscillation. *J. Atmos. Sci.* **53**, 3032–3045.

Becker, E. and Schmitz, G. 2001. Interaction between extratropical stationary waves and the zonal mean circulation. *J. Atmos. Sci.* **58,** 462–480.

Daley, R. 1991. *Atmospheric Data Analysis*. Cambridge University Press, Cambridge, UK, 460 pp.

Derber, J. and Bouttier, F. 1999. A reformulation of the background error covariance in the ECMWF global data assimilation system. *Tellus* **51A,** 195–221.

Gilbert, J. C. and Lemaréchal, C. 1989. Some numerical experiments with variable storage quasi-Newton algorithms. *Math. Prog.* **B25,** 407–435.

Gill, A. E. 1980. Some simple solutions for heat-induced tropical circulation. *Q. J. R. Meteorol. Soc.* **106**, 447–462.

Fisher, M. 2003. Background error covariance modelling. In: *Proceedings of the ECMWF Seminar on Recent Developments in Data Assimilation for Atmosphere and Ocean*, ECMWF, 8–12 September 2003, 45–63.

Kasahara, A. 1976. Normal modes of ultralong waves in the atmosphere. *Mon. Wea. Rev.* **104**, 669–690.

Lindzen, R. S. 1974. Wave-CISK in the Tropics. *J. Atmos. Sci.* **31**, 156–179.

Matsuno, T. 1966. Quasi-geostrophic motions in the equatorial area. *J. Meteor. Soc. Japan* **44**, 25–42.

Milliff, R. F. and Madden, R. A. 1996. The existence and vertical structure of fast, eastward-moving disturbances in the equatorial troposphere. *J. Atmos. Sci.* **53**, 586–597.

Parrish, D. F. and Derber, J. C. 1992. The National Meteorological Center's spectral statistical interpolation analysis system. *Mon. Wea. Rev.* **120**, 1747–1763.

Rossby, C. G. 1937. On the mutual adjustment of pressure and velocity distributions in certain simple current systems. I. *J. Mar. Res.* **1**, 15–28.

Rossby, C. G. 1938. On the mutual adjustment of pressure and velocity distributions in certain simple current systems. II. *J. Mar. Res.* **2**, 239–263.

Stoffelen, A., Pailleux, J., Källén, E., Vaughan, J. M., Isaksen, L., and co-authors. 2005. The atmospheric dynamic mission for global wind measurements. *Bull. Amer. Meteor. Soc.* **86**, 73–87.

Wheeler, M. and Kiladis, G. N. 1999. Convectively coupled equatorial waves: analysis of clouds and temperature in the wavenumber-frequency domain. *J. Atmos. Sci.* **56**, 374–399.

Wheeler, M., Kiladis, G. N. and Webster, P. J. 2000. Large-scale dynamical fields associated with convectively coupled equatorial waves. *J. Atmos. Sci.* **57**, 613–640.

Žagar, N., Gustafsson, N. and Källén, E. 2004. Variational data assimilation in the tropics: the impact of a background error constraint. *Q. J. R. Meteorol. Soc.* **130**, 103–125.

Žagar, N., Andersson, E. and Fisher, M. 2005. Balanced tropical data assimilation based on a study of equatorial waves in ECMWF short-range forecast errors. *Q. J. R. Meteorol. Soc.* **131**, 987–1011.